www.czasopisma.pan.pl PAN POLSKA AKADEMIA NAUK www.journals.pan.pl

INTL JOURNAL OF ELECTRONICS AND TELECOMMUNICATIONS, 2023, VOL. 69, NO. 1, PP. 69-74
Manuscript received December 2, 2022; revised January, 2023. DOI: 10.24425/ijet.2023.144333

Design and Development of Biodegradable 3D Printed RDRA for Polarization Reconfigurability

Maganti Apparao, and Godi Karunakar

***Abstract*—In this article, a 3D printed rectangular dielectric resonator antenna which is capable of polarization reconfiguration has been designed. Dielectric resonator is composed of environment friendly and biodegradable material, which is Polylactic Acid. In the proposed model, the polarization can be switch from a linear to a circular by changing the state of a switch, electonically. The antenna switch between two different polarizations: Linear polarization during OFF STATE and Left-hand circular polarization during ON STATE. The proposed 3D printed dielectric resonator antenna is designed to operate in C-band of microwave spectrum, with a broad effective bandwidth (overlapped impedance bandwidths of both states) of 14.542% with centre frequency at 5.845GHz and peak gain 5.5dBi. Further, validated simulated results with experiment and both results are in good agreement.**

***Keywords*—polarization switching; circular polarization; linear polarization; dielectric resonator antenna**

I. INTRODUCTION

POLARIZATION-RECONFIGURABLE antennas [1]-[5] get popularized in recent years. Polarization reconfiguration has been validated with several types of antennas, like monopole [6], dipole [7], aperture [8], and patch antennas [9]-[10] and these antennas have plenty of applications in wireless communication systems, such as modulation [11], diminishing fading losses which can be generated because of multipath effects [6], enhancing the attributes and channel capacity in a multiple input multiple output (MIMO) systems [12], and helps in minimizing the signal depolarization [13]. This helps in diminishing the polarization mismatch and as a result, it improves the Signal to Interference plus Noise Ratio (SINR). Mostly polarization reconfigurable antennas have the metallic radiators which result in Low radiation efficiency and narrow bandwidth because of conductor losses, skin effect, etc.

Dielectric resonator antennas (DRAs) have the distinct attribute that the dielectric radiators are used to radiate instead of metallic radiators. In the literature, several designs have been reported, for DRAs realizing various forms of reconfiguration such as in reference [14]-[16], liquid dielectrics were employed to reconfigure the: operating frequency [14], radiation pattern [15], and polarization [16] of DRAs. In this article, we proposed a 3D printed Rectangular DRA (RDRA), where polarization can be switch from linear to circular by changing the state of PIN diode. During OFF state of switch antenna behaves as a linearly polarized antenna and when the switch is in ON condition, antenna starts to behave as a circularly polarized antenna. 3D printed RDRA offer various advantages in comparison with the use of other dielectric materials such as light-weight, low cost, time-efficient, and small form-factor (SFF). 3D printing or Additive manufacturing is a method of fabricating 3D objects using layer-by-layer approach [17] and it enables to produce complex structures from a digital model. The proposed antenna was optimized for polarization reconfiguration, which was simply attained by altering the electromagnetic-field (EMF) distribution of the DRA. A switch was used to redistribute the EMF, which resulted in polarization reconfiguration.

The proposed antenna can operate in a broad effective bandwidth (overlapped bandwidths of the two operating states) of 14.542% with centre frequency at 5.845GHz.

II. ANTENNA DESIGN

The proposed Polarization reconfigurable Rectangular dielectric resonator (RDR) of Sides (DR_S) 17mm and Height (DR_H) 12mm is places at the centre of a square substrate of the Fr4 material having sides (S) of 50mm and thickness (T) of 1.6mm. The RDRA was fabricated with polymer material by utilizing additive manufacturing technology, which has a dielectric constant of 2.65 and loss tangent (tan δ) of 0.003. A square substrate has a finite ground plane, and a circular ring aperture has been etched out on the ground plane to electrify the RDRA via a 50Ω microstrip feed line of Length (FL) = 27mm, on the other side of substrate. The ring has 7mm of outer radius ($Outer_R$) and 5.7mm of inner radius ($Inner_R$). Two pins of radius 0.6mm was inserted after drilling, and connected with ground at position of (SW_P)= 90º from feed line. One pin was inserted inside the ring slot and another is inserted at outer side of ring slot and a switch has been implanted to short/open the connection between both pins.

One common approach to analyse a RDRA is the dielectric waveguide model (DWM) method. This method can estimate the resonance frequency of the DRA, but the error can be over 10% depending on the aspect ratio and dielectric constant of the DRA. Although rigorous numerical analysis can be used to accurately calculate the resonance frequency and field by simulation software, HFSS has been used to optimize the proposed 3D printed polarisation reconfigurable antenna system.

Authors are with Department of Electronics and Communication Engineering, Gitam Institute of Technology, GITAM Deemed to be University, Visakhapatnam, India (e-mail: magantiaprao@gmail.com, profkarunakar @gmail.com).

The theoretical formula for resonant frequency (f_r) of an RDRA is given as:

$$f_r = \frac{c}{2\pi\sqrt{\varepsilon_r}}\sqrt{k_x^2 + k_y^2 + k_z^2} \quad (1)$$

where "ε_r" is the dielectric constant of the RDRA, "c" is the speed of light in free space and symbol "k_x", "k_y" and "k_z" represents the wavenumbers in the x, y and z directions respectively.

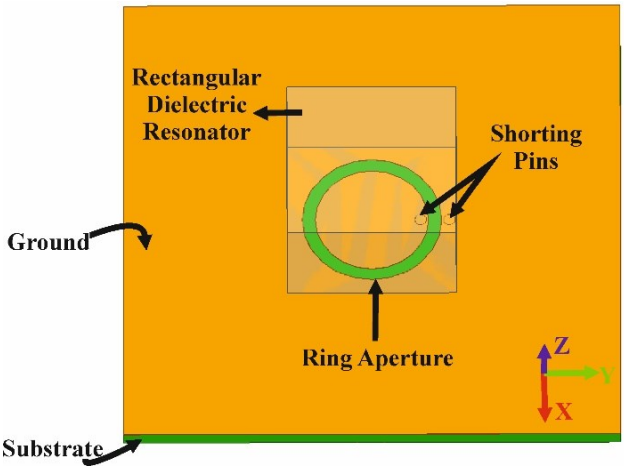

(a) Top View

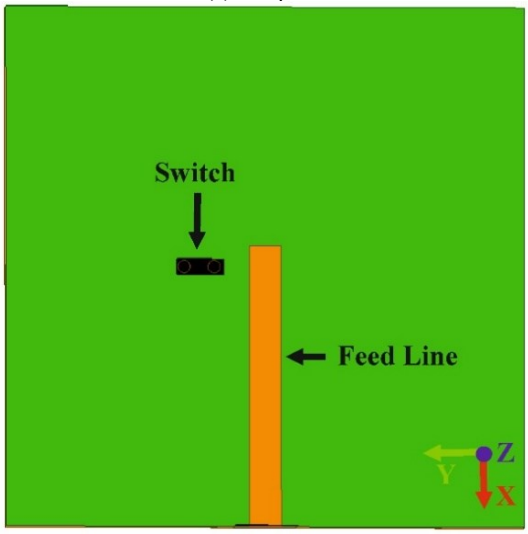

(b) Bottom View

Fig. 1. Illustration of Proposed Antenna

Initially, Antenna dimensions of DR_S= 15mm and DR_H=15mm, $Outer_R$= 8mm, $Inner_R$= 6mm was adopted, then different parameters such as DR_S, DR_H, $Outer_R$, $Inner_R$, and SW_P was optimized to improved impedance matching in C band, and at the value of $Outer_R$= 7mm, $Inner_R$= 5.7mm improvement was noticed. First DR_H was optimized when DR_S= 15mm, $Outer_R$= 7mm, $Inner_R$= 5.7mm and FL= 27mm. The $|S_{11}|$ of different dimension of DR_H is shown in Fig. 2.

later DR_S was optimised when DR_H= 18mm, $Outer_R$= 7mm, $Inner_R$= 5.7mm and FL= 27mm. The $|S_{11}|$ of different dimension of DR_H is shown in Fig. 3, and it can be concluded from Fig.2 and Fig.3 that at DR_H= 18mm and DR_S = 20mm DRA was best coupled with transmission line.

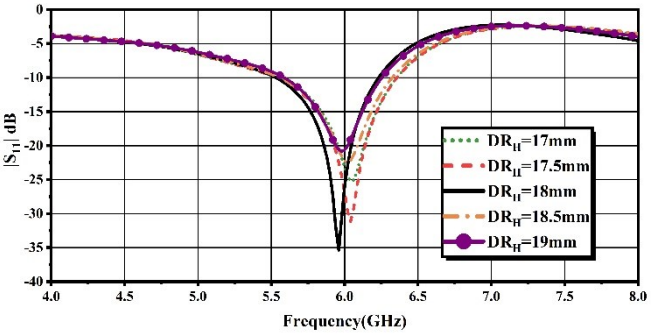

Fig. 2. Simulated $|S_{11}|$ of different dimension of DR_H when DR_S = 15mm, $Outer_R$ = 7mm, $Inner_R$ = 5.7mm and FL = 27mm

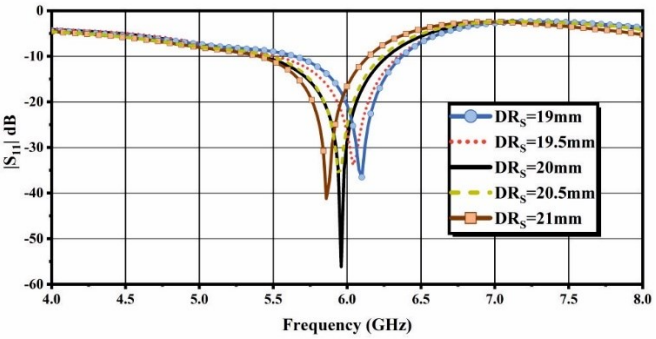

Fig. 3. Simulated $|S_{11}|$ of different dimension of DR_S when DR_H= 18mm, $Outer_R$= 7mm, $Inner_R$= 5.7mm and FL= 27mm

Later, at SW_P= 90º from the feed line, a switch has been implemented to short the ring. The simulated $|S_{11}|$ and Axial ratio (AR), when switch is in ON state are depicted in Fig. 4 and Fig. 5 for DR_H= 18mm, DR_S= 20mm, $Outer_R$= 7mm, $Inner_R$= 5.7mm and FL= 27mm. After introducing switch into the system, slight changes in operating bandwidth of $|S_{11}|$ has been observed, and it is because of the implementation of active component into the substrate. It was also observed that, DR was coupled perfectly at DR_H=18 as well as DR_S=20mm and bandwidth of $|S_{11}| \leq$ -10dB is greater when switch is in ON state than the bandwidth when switch is in OFF state. The operating band and frequency for AR ≤ 3dB can be shift by changing the angular position of switch and it can be note from Fig. 6, which depict the AR for different values of SW_P, but if we notice the reflection coefficient in Fig. 7, it can be easily conclude that the reflection of power is minimum at SW_P=90º.

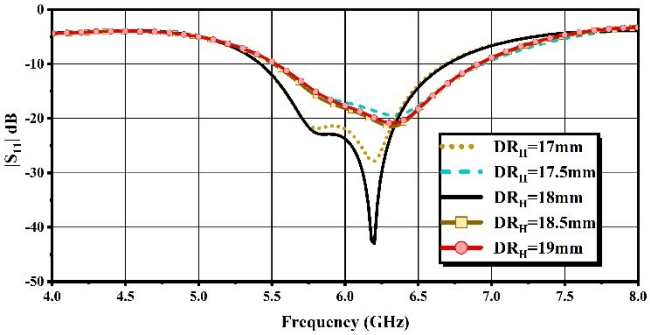

(a) Simulated $|S_{11}|$ for different values of DR_H when switch is in ON state

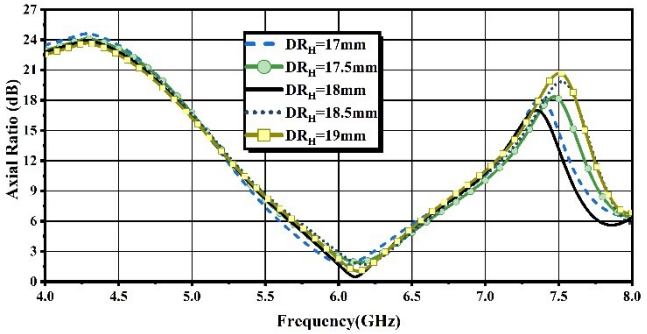

(b) Simulated Axial Ratio for different values of DR_H when switch is in ON state.

Fig. 4. Simulated $|S_{11}|$ and Axial Ratio for different values of DR_H.

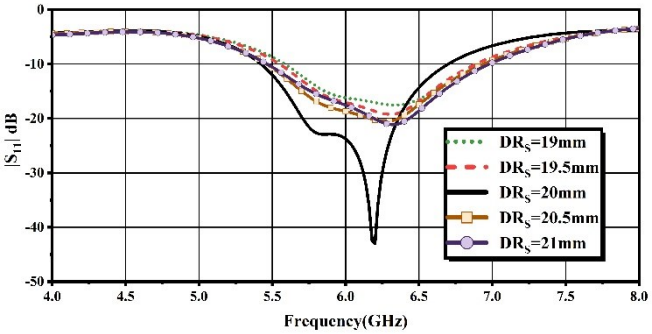

(a) Simulated $|S_{11}|$ for different values of DR_S when switch is in ON state

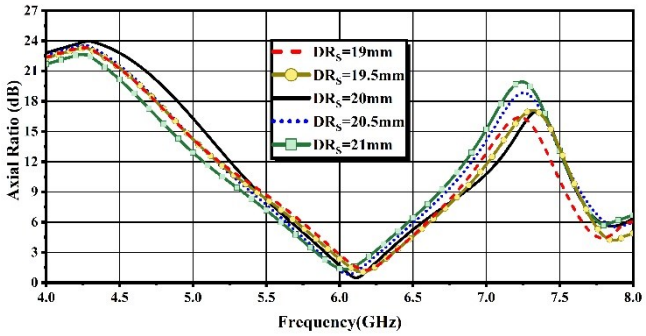

(b) Simulated Axial Ratio for different values of DR_S when switch is in ON state

Fig. 5. Simulated $|S_{11}|$ and Axial Ratio for different values of DR_S.

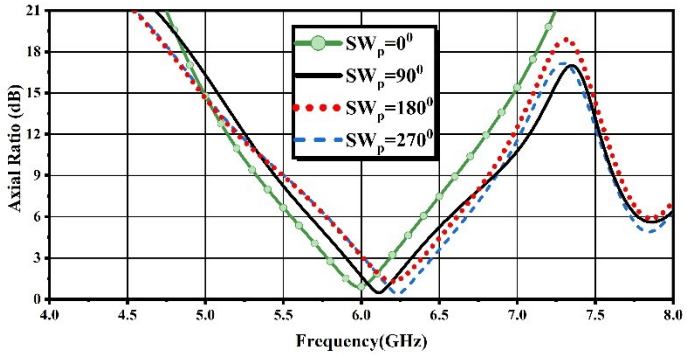

Fig. 6. Simulated Axial Ratio for different values of SW_P when switch is in ON state

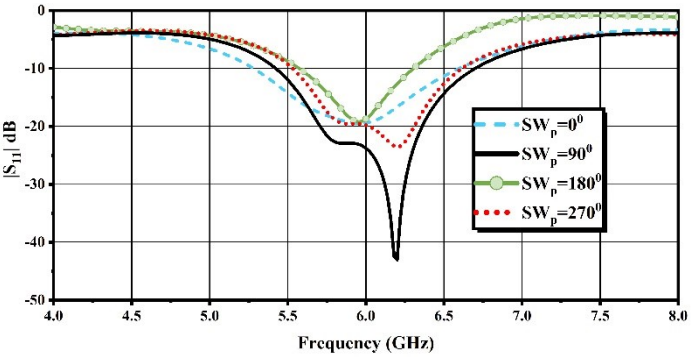

Fig. 7. Simulated $|S_{11}|$ for different values of SW_P when switch is in ON state.

The Far filed properties are very important parameter to check, and the radiation pattern has also been studied and it can be observed from Fig. 8 to Fig. 11 that the radiation pattern is stabilized while operating in both the states. From Fig. 10 and Fig. 11 of normalized radiation pattern, it can be notice that radiation is left hand circular polarization (LHCP), when switch is ON. The proposed antenna can work in both linear and circular polarization so gain vs frequency and AR has been depicted in Fig. 12 and Fig. 13 respectively.

The polarization can be switch from linear to circular by changing the state of switch. In OFF state antenna will work as linearly polarized antenna and in ON state antenna will work as Circular polarized antenna. The summarized results are shown in Fig. 12 and Fig. 13.

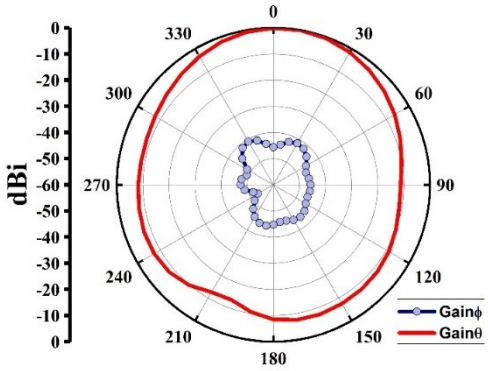

Fig. 8. Simulated Normalized radiation pattern when switch is OFF at E-plane

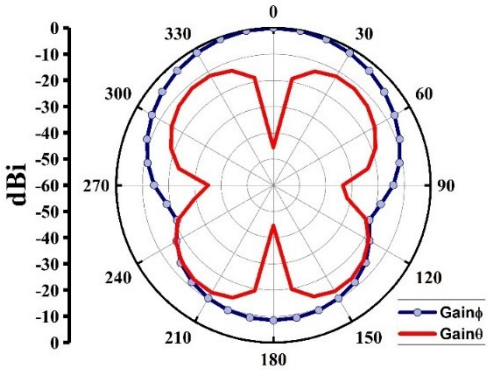

Fig. 9. Simulated Normalized radiation pattern when switch is OFF at H-plane

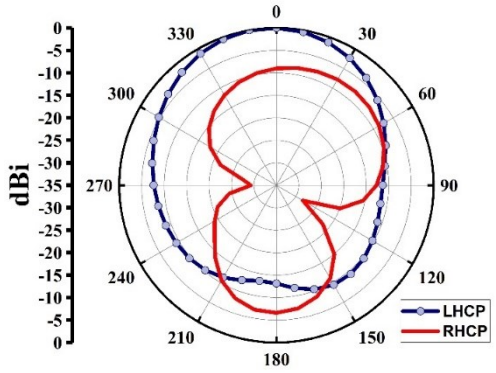

Fig. 10. Simulated Normalized radiation pattern when switch is ON at E-plane

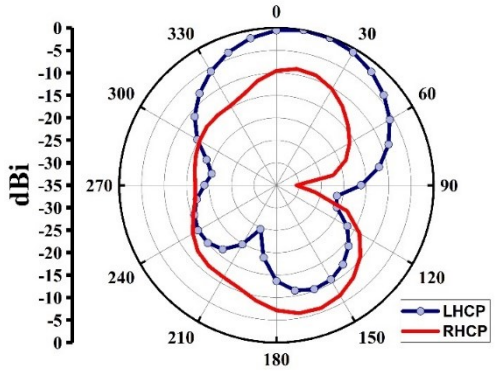

Fig. 11. Simulated Normalized radiation pattern when switch is ON at H-plane

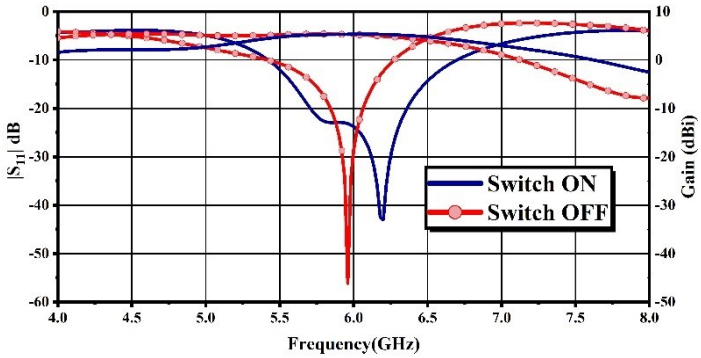

Fig. 12. Simulated $|S_{11}|$ and Gain when switch is in ON and OFF state

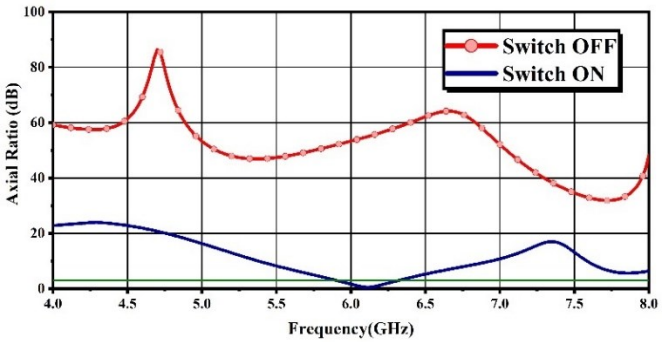

Fig. 13. Simulated Axial ratio when switch is in ON and OFF state

III. Results and Analysis

To validate this idea of polarization reconfigurable antenna, a prototype of proposed antenna was developed and verified experimentally. The photograph of fabricated RDRA is shown in Fig. 14 which is developed by using a 3D printer. Chip resistors of two different values are used to realization the ON and OFF conditions. The value of the chip resistor is 0.001 kΩ and 3 kΩ for ON and OFF switching conditions respectively. The reflection coefficient has been measured using an E8364B PNA network analyser and it can be noticed that there is a slight shift of operating band and resonant frequency because of the integration of the active components in Fig. 15 and summarized in Table I. The measurement of the far-field characteristics was measured using a Compact Antenna Test Range (CATR) setup, the simulated and measured far-field characteristics are depicted in Fig. 16 to Fig. 21.

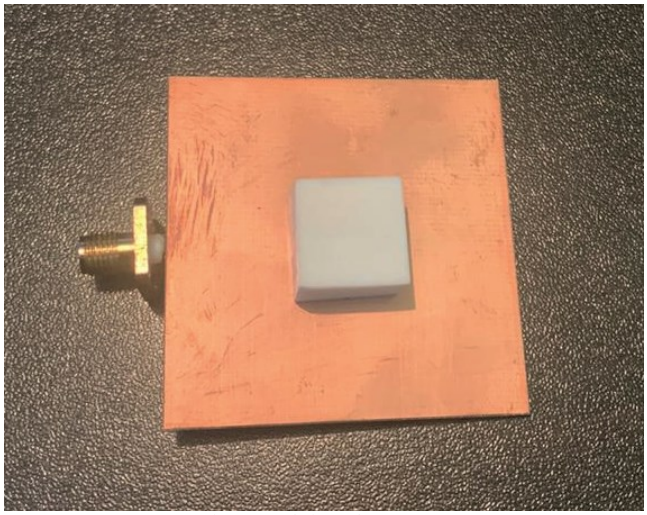

Fig. 14. Fabricated Prototype

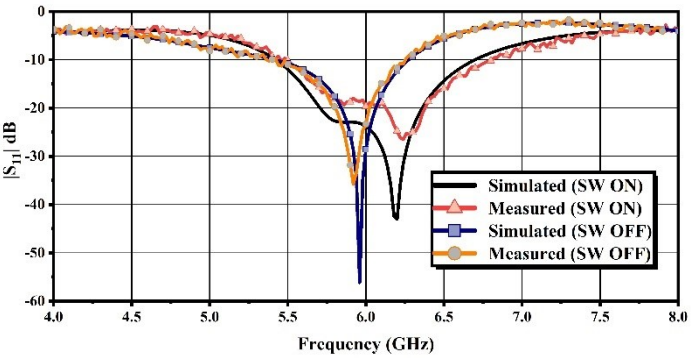

Fig. 15. Simulated and Measured reflection coefficient

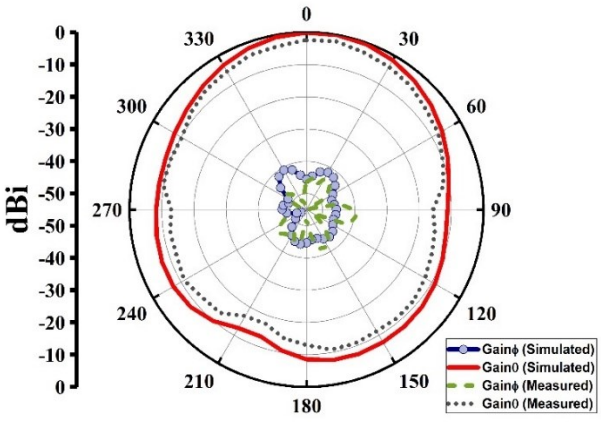

Fig. 16. Simulated and Measured Normalized radiation pattern when switch is OFF at E-plane

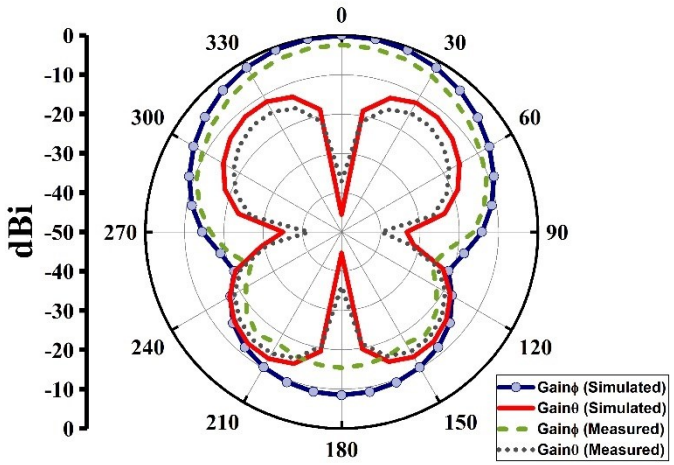

Fig. 17. Simulated and Measured Normalized radiation pattern when switch is OFF at H-plane

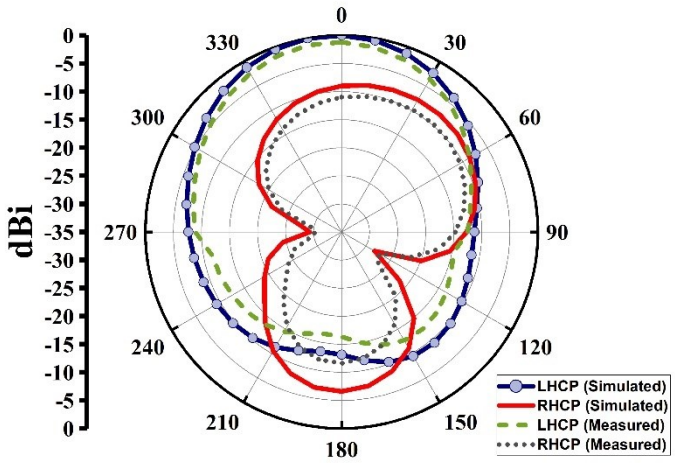

Fig. 18. Simulated and Measured Normalized radiation pattern when switch is ON at E-plane

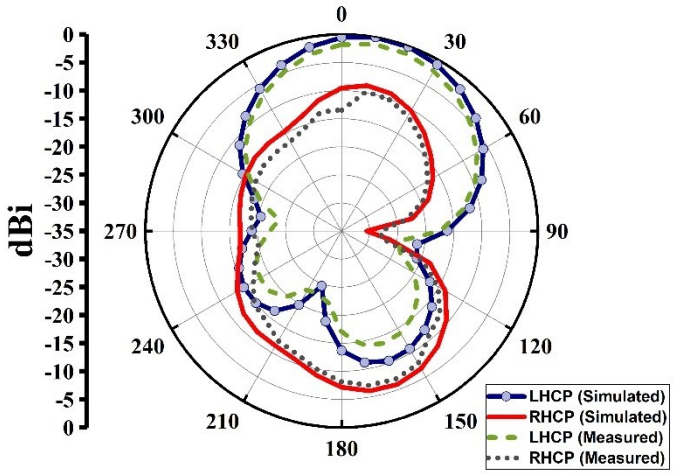

Fig. 19. Simulated and Measured Normalized radiation pattern when switch is OFF at H-plane

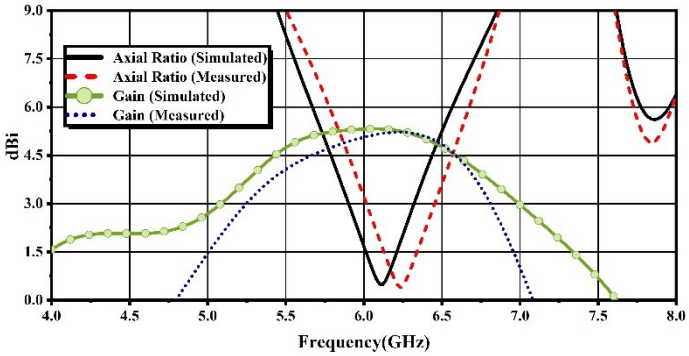

Fig. 20. Simulated and Measured Axial Ratio as well as Peak gain when switch is ON

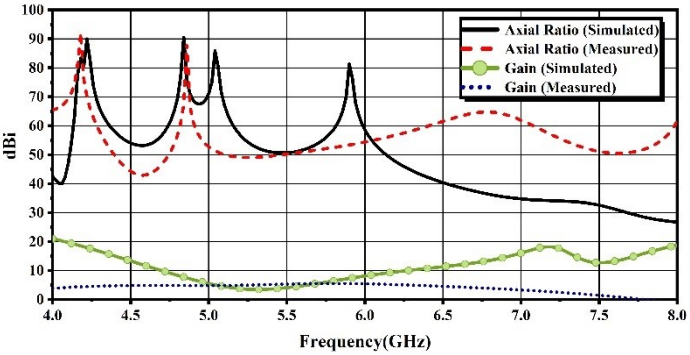

Fig. 21. Simulated and Measured Axial Ratio as well as Peak gain when switch is OFF.

Table I
SIMULATED AND MEASURED RESULTS OF PROPOSED POLARIZATION RECONFIGURABLE 3D PRINTED RDRA

	Pol.	Switch State	R.C. B.W. (GHz)	A.R. B.W. (GHz)	Peak Gain (dBi)
Simulated	Circular	ON	5.47 -6.8	5.91 - 6.32	5.35
	Linear	OFF	5.42 -6.7	5.42 - 6.7	5.48
Measured	Circular	ON	5.42 -6.27	6.01 - 6.45	5.2
	Linear	OFF	5.37 -6.25	5.37 - 6.25	5.52

R.C.- Reflection Coefficient, B.W.- Bandwidth, A.R.- Axial Ratio.

Table I summarized the simulated and measured results of proposed polarization reconfigurable 3D printed RDRA. It can be observed from Fig. 15 as well that the operating band of $|S_{11}| \leq$ -10dB has been shifted in both cases i.e. when switch is ON and when switch is OFF, but the operating bandwidth is almost identical. The simulated and measured radiation patterns of both states are normalized and plotted in Fig. 16 to Fig. 21 and slight difference in radiation pattern was also observed, but peak gain was almost identical as of simulated. The measured Axial ratio bandwidth of antenna when switch is in ON state can be noticed in Fig. 20, and it can be easily concluded that operating band for A.R.$\leq$ 3dB is almost same but the operating frequencies are slightly shifted. The performance of proposed polarization reconfigurable 3D printed RDRA is compared with other different type of polarization reconfigurable antenna in Table II.

Table II
COMPARISON OF PROPOSED POLARIZATION RECONFIGURABLE 3D PRINTED RDRA WITH OTHER DIFFERENT TYPE OF POLARIZATION RECONFIGURABLE

	Pol.	Switch State	R.C. B.W. (GHz)	A.R. B.W. (GHz)	Peak Gain (dBi)
[1]	Circular	ON	2.49-2.58	2.49-2.58	5.8
	Linear	OFF	2.41-2.75	2.41-2.75	6.2
[2]	Circular	ON	2.18-2.75	2.45-2.57	6.5
	Linear	OFF	2.37-2.6	2.37-2.6	7
[3]	LHCP	ON	2.47-3.04	2.58-2.69	4.76
	RHCP	OFF	2.45-3.01	2.58-2.68	3.1
P.A.	Circular	ON	5.47 -6.8	6.01 - 6.45	5.2
	Linear	OFF	5.37 - 6.25	5.37 - 6.25	5.52

P.A.- Proposed Antenna, R.C.- Reflection Coefficient, B.W.- Bandwidth, A.R.- Axial Ratio.

IV. CONCLUSION

This article presents a 3D printed polarization-reconfigurable RDRA. The antenna is able to switch its polarization between linear and circular. The measurements and simulations were in good agreement. The proposed antenna has a broad effective bandwidth of 14.542% with centre frequency at 5.845GHz. In addition, it has a stable gain and then most reported reconfigurable DRAs incorporating p-i-n-diodes. For a potential application, the 3D printed reconfigurable RDRA could be used within a wireless detection system where different information is transmitted on different channels differing in their polarizations.

REFERENCE

[1] J. S. Row and R. H. Chen, "Reconfigurable slot-coupled microstrip antenna with polarization diversity," *IET Microw. Antennas Propag.*, vol. 1, no. 3, pp. 798–802, Jun. 2007. http://doi.org/10.1049/iet-map:20060184

[2] J. S. Row and J. F. Wu, "Aperture-coupled micorstrip antennas with switchable polarization," *IEEE Trans. Antennas Propag.*,vol. 54, no. 9, pp. 2686–2691, Sep. 2006. http://doi.org/10.1109/TAP.2006.880785

[3] J. F. Wu and J. S. Row, "Broadband circularly-polarised microstrip antenna with switchable polarization sense," *Electron. Lett.*, vol. 42, no. 24, pp. 1374–1375, Nov. 2006. http://doi.org/10.1049/el:20063065

[4] Y. J. Kim, J. K. Kim, J. H. Kim, and H. M. Lee, "Reconfigurable annular ring slot antenna with circular polarization diversity," in *Proc. Asia-Pacific Microw. Conf.*, Bangkok, Thailand, 2007, pp. 1–4. http://doi.org/10.1109/APMC.2007.4554837

[5] M. K. Fries, M. Grani, and R. Vahldieck, "A reconfigurable slot antenna with switchable polarization," *IEEE Microw. Wireless Comp. Lett.*, vol. 13, no. 11, pp. 490–492, Nov. 2003. http://doi.org/10.1109/LMWC.2003.817148

[6] B. Liang, B. Sanz-Izquierdo, E. A. Parker and J. C. Batchelor, "A frequency and polarization reconfigurable circularly polarized antenna using active EBG structure for satellite navigation," *IEEE Trans. Antennas Propag.*, vol. 63, no. 1, pp. 33-40, Jan. 2015. http://doi.org/10.1109/TAP.2014.2367537

[7] W. Yang, W. Che, H. Jin, W. Feng and Q. Xue, "A polarization-reconfigurable dipole antenna using polarization rotation AMC structure," *IEEE Trans. Antennas Propag.*, vol. 63, no. 12, pp. 5305-5315, Dec. 2015. http://doi.org/10.1109/TAP.2015.2490250

[8] Y. Li, Z. Zhang, W. Chen and Z. Feng, "Polarization reconfigurable slot antenna with a novel compact CPW-to-slotline transition for WLAN application," *IEEE Antennas Wireless Propag. Lett.*, vol. 9, pp. 252-255, 2010. http://doi.org/10.1109/LAWP.2010.2046006

[9] P. Y. Qin, A. R. Weily, Y. J. Guo and C. H. Liang, "Polarization reconfigurable U-slot patch antenna," *IEEE Trans. Antennas Propag.*, vol. 58, no. 10, pp. 3383-3388, Oct. 2010. http://doi.org/10.1109/TAP.2010.2055808

[10] S. L. Chen, F. Wei, P. Y. Qin, Y. J. Guo and X. Chen, "A multi-linear polarization reconfigurable unidirectional patch antenna," *IEEE Trans. Antennas Propag.*, vol. 65, no. 8, pp. 4299-4304, Aug. 2017. http://doi.org/10.1109/TAP.2017.2712185

[11] M. A. Kossel, R. Kung, H. Benedickter and W. Biichtokd, "An active tagging system using circular-polarization modulation," *IEEE Trans. Microw. Theory Tech.*, vol. 47, no. 12, pp. 2242-2248, Dec. 1999. http://doi.org/10.1109/22.808966

[12] J. F. Valenzuela-valdes, M. A. Garcia-fernandez, A. M. Martinez-gonzalez and D. Sanchez-Hernandez, "The role of polarization diversity for MIMO systems under rayleigh-fading environments," *IEEE Antennas Wireless Propag. Lett.*, vol. 5, no. 1, pp. 534-536, Dec. 2006. http://doi.org/10.1109/LAWP.2006.889552

[13] H. Wong, W. Lin, L. Huitema and E. Arnaud, "Multi-polarization reconfigurable antenna for wireless biomedical system," *IEEE Trans. Biomed. Circuit Syst.*, vol. 11, no. 3, pp. 652-660, June 2017. http://doi.org/10.1109/TBCAS.2016.2636872

[14] G. H. Huff, D. L. Rolando, P. Walters and J. McDonald, "A frequency reconfigurable dielectric resonator antenna using colloidal dispersions," *IEEE Antennas Wireless Propag. Lett.*, vol. 9, no., pp. 288-290, 2010. http://doi.org/10.1109/LAWP.2010.2046613

[15] [10] Z. Chen and H. Wong, "Wideband glass and liquid cylindrical dielectric resonator antenna for pattern reconfigurable design," *IEEE Trans. Antennas Propag.*, vol. 65, no. 5, pp. 2157-2164, May 2017. http://doi.org/10.1109/TAP.2017.2676767

[16] [11] Z. Chen and H. Wong, "Liquid dielectric resonator antenna with circular polarization reconfigurability," *IEEE Trans. Antennas Propag.*, vol. 66, no. 1, pp. 444-449, Jan. 2018. http://doi.org/10.1109/TAP.2017.2762005

[17] R. C. Rumpf, J. Pazos, C. R. Garcia, L. Ochoa, and R. Wicker, "3D printed lattices with spatially variant selfcollimation," *Progr. Electromagnet. Res.*, Vol. 139, pp. 1–14, Mar. 2013. http://doi.org/10.2528/PIER13030507